3541

Accurate mUlti-echo phase image wiTh uneven echO spacing and Ultra-High Dynamic Range (AUTO-HDR)

Yuheng Huang[1,2], Xinheng Zhang[1,2], Serry Fradad[1], Lu Meng[1], Ghazal Yoosefian[1], Linda Azab[1], Xinqi Li[3], Alan Kwan[4], Rohan Dharmakumar[1], Hui Han[1], and Hsin-Jung Yang[1]

[1]Biomedical Imaging Research Institute, Cedars Sinai Medical Center, Los Angeles, CA, United States, [2]Bioengineering, UCLA, Los Angeles, CA, United States, [3]Columbia University, New York, NY, United States, [4]Cardiology, Cedars Sinai Medical Center, Los Angeles, CA, United States

Synopsis

A strong off-resonance field around metallic implants induces unreliable phase maps and limits the application of phase-based MRI techniques. State-of-the-art MR phase mapping and unwrapping techniques perform poorly under the influence of metallic implants because of their limited dynamic range and susceptibility to noise. In this study, we developed a fully automatic phase mapping technique based on a multi-echo GRE sequence with unevenly spaced echoes and a high-dynamic-range phase reconstruction algorithm. We tested the proposed method with numerical simulations and human subjects with metallic implants.

Introduction

Recent technical advancements in phase-based MRI applications, such as susceptibility imaging, flow-encoded imaging, and B0 field mapping, have demonstrated major clinical values in diagnosis, pathophysiological research, and image quality improvement.[1, 2] The accurate derivation of the phase terms in MR images serve as the foundation of these modalities. However, accompanied by the uprising popularity of high field MRI scanner and MRI safe metallic implants, strong B0 field inhomogeneity around metallic implants became a common confounder in phase map derivation. The strong B0 off-resonance induced by the metallic objects drastically impairs the accuracy, reliability, and applicability of the phase-based MRI techniques, particularly in the regions with strong phase accumulation and multi-fold phase wrapping. Although algorithms had been proposed to unwrapping MR phase images,[3,4,5] the state-of-the-art algorithms were not suitable for the extreme conditions of the presents of metallic implants and are confounded by limited phase dynamic range and high susceptibility to noise. These challenges result in significant phase wrapping artifacts, shifted central frequency and unreliable against sudden phase changes at fat/water interfaces. In this study, we proposed a new phase processing algorithm, named "Accurate mUlti-echo phase image wiTh uneven echO spacing and Ultra-High Dynamic Range (AUTO-HDR)", that is robust against noise and is able to resolve ultra-high dynamic range to the level of off-resonance near metallic implants. We tested the proposed methods in numerical phantoms and compared them with four other state-of-the-art phase unwrapping techniques. We also validated the results in human subjects with an implantable cardioverter-defibrillator on their chest.

Method

The image processing pipeline of AUTO-HDR is depicted in Fig.1A. A multi-echo GRE(mGRE) sequence with unevenly spaced echoes was adopted(Fig.1B) to create an extended dynamic range for the phase maps.[6,7] To achieve a higher dynamic range, a graph-cut based algorithm was used and guided by the second temporal derivative phase images to utilize the high SNR in long TE images and preserve the accurate and reliable unwrapping property from the images with short TEs. To validate the proposed method, a numerical simulation, and in-vivo experiments were performed and described as the following: Numerical Phantom: Based on the regularized inversion method,[8] a numerical phantom was generated with a shepp-logan model[9] and a common metallic object (implantable cardioverter-defibrillator; ICD Medtronic VISIA AF), size. The position of imaging FOV, ferromagnetic object, and the induced field map is illustrated in Fig 2A. Images were simulated under different SNR levels to emulate the imaging condition.[10] An mGRE sequence with the following experimental setups was simulated based using the Bloch equation to generate the corresponding complex images. TE:(1.07, 3.07, 5.27,7.67)ms; TR:1124.67ms ; FOV:360*125*96mm^3; Voxel Size:1.607*1.607*3.214mm^3. Repeated experiments (N=20) were conducted to test the robustness and reproducibility of the algorithms. All images were processed with AUTO-HDR and four other state-of-the-art phase unwrapping techniques (Quality Guide, SPURS, UMPIRE, and LAPLACIAN). The quality of the phase maps was measured quantitatively in an ROI close to the off-resonance source(Fig. 2B). Normalized Root Means Square Error (NRMSE) and SD of error maps was measured in the ROI and compared using bar plots. In-vivo experiment: To further validate the simulated results, an in-vivo experiment was performed at a clinical 3T scanner (mMR, Siemens). A human volunteer with a metallic off-resonance source(implantable cardioverter-defibrillator; ICD) on the left anterior chest wall was scanned with the same imaging parameter. 3D mGRE Images were acquired with a 25-sec breath-hold and covering the whole chest.

Results

Numerical Phantom: Fig.3 showed the results from unwrapped phase maps of the numerical phantom under different noise levels. Phase maps derived using AUTO-HDR and four other state-of-the-art unwrapping algorithms were compared with the theoretical inputs, and error maps were derived. In the area close to the off-resonance source, SPURS, Laplacian, and Quality Guided with long TE(DTE=6.4ms), showed strong error in determining the central frequency of the phase maps. Although quality Guided images using short TE(DTE=2ms) and UMPIRE can achieve correct central frequencies, the strong amplification of noise corrupted the images significantly, particularly in the region close to the off-resonance source. The proposed AUTO-HDR, however, was able to unwrap the images in the whole FOV and performed robustly against different noise levels. Similar trends were observed in the quantitative analysis(Fig.4). The proposed method showed unparallel robustness compare to the other algorithms and demonstrated significantly lower RMSE and higher SNR at the ROI under various noise levels. In-vivo experiment: Similar results to the simulation are presented in the in-vivo experiment(Fig 5). Improved phase wrapping artifacts, off-centered central frequency and lower noise level are shown with the proposed AUTO-HDR compare to the peer algorithms.

Conclusion

AUTO-HDR can accurately estimate MRI phase maps under the presence of metallic implants. It demonstrates superior accuracy and robustness compare to the state-of-the-art algorithms under insufficient SNR, and ultra-high off-resonance range. A more comprehensive study on more human subjects with quantitative measures is needed to exam its in-vivo reliability.

Acknowledgements

References

1.Haacke EM, Mittal S, Wu Z, Neelavalli J, Cheng YC. Susceptibility-weighted imaging: technical aspects and clinical applications, part 1. AJNR Am J Neuroradiol. 2009 Jan;30(1):19-30. doi: 10.3174/ajnr.A1400. Epub 2008 Nov 27. PMID: 19039041; PMCID: PMC3805391.

2. Juchem C, Umesh Rudrapatna S, Nixon TW, de Graaf RA. Dynamic multi-coil technique (DYNAMITE) shimming for echo-planar imaging of the human brain at 7 Tesla. Neuroimage. 2015 Jan 15;105:462-72. doi: 10.1016/j.neuroimage.2014.11.011. Epub 2014 Nov 8. PMID: 25462795; PMCID: PMC4262558.

3. K Bartusek et al 2006 Meas. Sci. Technol. 17 3293

4. Robinson SD, Bredies K, Khabipova D, Dymerska B, Marques JP, Schweser F. An illustrated comparison of processing methods for MR phase imaging and QSM: combining array coil signals and phase unwrapping. NMR Biomed. 2017 Apr;30(4):e3601. doi: 10.1002/nbm.3601. Epub 2016 Sep 13. PMID: 27619999; PMCID: PMC5348291.

5. Dong J, Liu T, Chen F, Zhou D, Dimov A, Raj A, Cheng Q, Spincemaille P, Wang Y. Simultaneous phase unwrapping and removal of chemical shift (SPURS) using graph cuts: application in quantitative susceptibility mapping. IEEE Trans Med Imaging. 2015 Feb;34(2):531-40. doi: 10.1109/TMI.2014.2361764. Epub 2014 Oct 8. PMID: 25312917.

6. Robinson S, Schödl H, Trattnig S. A method for unwrapping highly wrapped multi-echo phase images at very high field: UMPIRE. Magn Reson Med. 2014 Jul;72(1):80-92. doi: 10.1002/mrm.24897. Epub 2013 Jul 30. PMID: 23901001; PMCID: PMC4062430.

7. Dagher J, Reese T, Bilgin A. High-resolution, large dynamic range field map estimation. Magn Reson Med. 2014 Jan;71(1):105-17. doi: 10.1002/mrm.24636. Epub 2013 Feb 11. PMID: 23401245; PMCID: PMC3919137.

8. Shi X, Yoon D, Koch KM, Hargreaves BA. Metallic implant geometry and susceptibility estimation using multispectral B0 field maps. Magn Reson Med. 2017 Jun;77(6):2402-2413. doi: 10.1002/mrm.26313. Epub 2016 Jul 6. PMID: 27385493; PMCID: PMC5529184.

9. H. M. Gach, C. Tanase and F. Boada, "2D & 3D Shepp-Logan Phantom Standards for MRI," 2008 19th International Conference on Systems Engineering, Las Vegas, NV, 2008, pp. 521-526, doi: 10.1109/ICSEng.2008.15.

10. Rashid S, Rapacchi S, Vaseghi M, Tung R, Shivkumar K, Finn JP, Hu P. Improved late gadolinium enhancement MR imaging for patients with implanted cardiac devices. Radiology. 2014 Jan;270(1):269-74. doi: 10.1148/radiol.13130942. Epub 2013 Oct 28. PMID: 24086074; PMCID: PMC4228714.
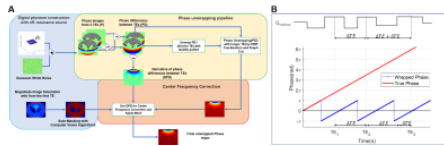
Figures

Figure 1. Image processing flow chart and the uneven echo spacing. The image processing pipeline is presented in panel A. Phase images were first combined with a graph-cut algorithm to conduct high SNR phase maps. The central frequency and unwrapping artifact were further calibrated from the derivative of the phase difference maps between the uneven DTEs. The phase accumulation from the uneven echo spacing is presented in panel B.
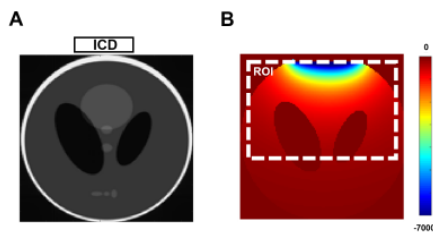

Figure 2. Experimental setting of the digital phantom. The relative location of the ICD and Shepp-logan phantom are presented in panel A. Panel B shows the representative off-resonance map induced by the simulated ICD. The region labeled with the white box was used to quantitatively evaluate the performance of the unwrapping algorithms.
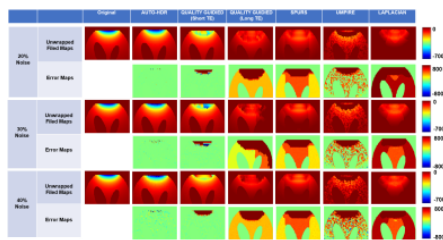

Figure 3. Unwrapped field maps and Error maps from different phase unwrapping algorithms. Phase images reconstructed with different algorithms are presented. Strong unwrapping artifacts and frequency shifts are shown in the peer unwrapping algorithms (columns 3-7) due to the susceptibility to noise and fast-changing local off-resonance field. The phase errors are reduced significantly by the proposed algorithm (AUTO-HDR; column 2), which presents near-identical maps to the input phase maps(column 1).
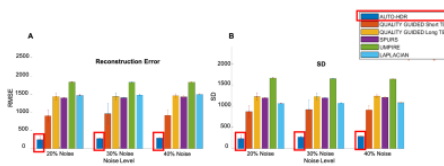

Figure 4. Comparison of reconstruction Error and noise level between phase unwrapping algorithms. Quantitative measurements of the root mean square error (panel A) and Standard deviation of the error map(panel B) are presented. AUTO-HDR shows significantly lower Error and noise level compare to the peer algorithms.
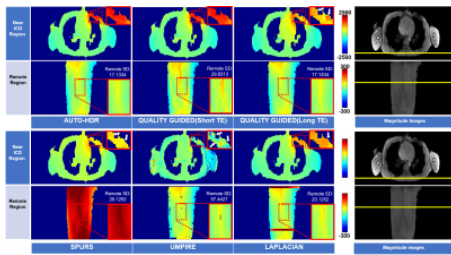
Figure 5. In-vivo images from a healthy human volunteer with an ICD on the chest. In the presents of ICD, the compromised image SNR and strong phase accumulation from the off-resonance source lead to obvious phase unwrapping artifacts and central frequency shifts in the peer algorithms (arrows). The proposed AUTO-HDR shows a much smoother field map around the ICD and higher SNR at a region further away from the ICD. The improved field map demonstrates the capability of AUTO-HDR in resolving fast varying phase change while preserving high SNR in human subjects with metallic implants.